Feasibility Evaluation of Thoracic CT Automatic Segmentation for Malignant Pleural Mesothelioma Treatment

Mitchell Chen[a], Emma Helm[b], Niranjan Joshi[a], Michael Brady[a] and Fergus Gleeson[b] *

[a] Medical Vision Laboratory, University of Oxford
[b] Department of Radiology, Churchill Hospital, Oxford

Abstract. Malignant Pleural Mesothelioma (MPM) is a form of aggressive tumour that is almost always associated with prior exposure to asbestos. Thoracic CT scans are typically used for evaluating response to chemotherapy treatment in patients with MPM. Currently, clinicians rely on visual analysis or manual measurement for quantifying the progression of the disease. To improve the efficiency and accuracy of this response assessment, we aim to develop an automatic segmentation algorithm. Our observations suggest that key difficulties include the complexity of tissue geometry and similarity in different tissue attenuation values in a thoracic scan. These potential challenges rules out the direct application of existing segmentation algorithms. We present a novel approach to the problem using the Non-Parametric Windows method to estimate the probability density functions of intensity values. These estimates can then be applied to assist automatic segmentation. Results of a semi-automatic segmentation algorithm are presented with insights into ways in which a fully-automatic segmentation can be developed.

1 Introduction

Malignant Pleural Mesothelioma (MPM) is a form of aggressive tumour that is almost always associated with prior exposure to asbestos, which has been historically used widely in the construction and manufacturing industries. Most Western governments have banned or limited use of this material. However, because there is a long latent period between exposure to asbestos and development of mesothelioma (typically 15-40 years), the incidence of the disease continues to rise in many parts of the world.

In MPM, the tumour arises from the pleural surface, the thin membrane coating the lung and chest wall. Common symptoms include: shortness of breath, weight loss and chest wall pain due to chest wall invasion and the accumulation of fluid in the pleural space. MPM poses a serious threat to public health. In the UK alone, over 1,800 people were diagnosed with MPM in 2008. The incidence of MPM ranges from 7-40 per million in developed countries [1]. Given the gradual phasing out of asbestos production in the 1980s and the disease's long latent period, it is expected the incidence of mesothelioma in the UK will continue to increase and ultimately peak in 2020 [2]. Currently the incidence is much lower in developing countries. In China for example, the current incidence is only 4 per million [3]. However, given China's large population and the fact that asbestos production in the country is still rising, MPM is likely to emerge as a more serious health concern in the years to come. Moreover the average age of developing the disease in developed countries is 60 years, whereas in China it is 45.2 years [3]. This may suggest an earlier and more widespread frequent exposure to asbestos in this country.

The diagnosis of MPM continues to be challenging. Most patients present with advanced disease and therefore treatment is often limited to palliation. The tumour generally has a very poor prognosis with a median survival of less than one year and five year survival of less than 1% [1]. Palliative treatment often involves chemotherapy. Despite the lack of a curative treatment, recent advances [4] based on a combination therapy have shown considerable promise in terms of progression-free survival. A typical patient journey for mesothelioma diagnosis and treatment is illustrated in Fig. 1. CT has been established as an effective imaging technique for the evaluation of MPM [5]. However, CT imaging has several limitations in terms of assessing tumour volume and growth. This is because tissues in the thorax (e.g consolidated lung, pleural effusion) often have similar attenuation to the primary tumour; rendering segmentation of tumour from surrounding structures problematic. When clinicians look at scans of patients with mesothelioma, additional features such as texture, heterogeneity and knowledge of normal anatomy are frequently taken into account.

Assessment of a disease's response to therapy is essential for the evaluation of clinical trials. This necessitates the quantification of tumour size and establishment of a standard tumour response criteria based on such measurements. The World Health Organization (WHO) first recommended a bidimensional quantification method; later the more widely used Response Evaluation Criteria in Solid Tumours (RECIST) guidelines were proposed, suggesting the use of a unidimensional quantity; the longest diameter of the lesion [6]. However, when applying RECIST to MPM, selection of measurement sites poses a major challenge and criteria may be applied differently by different investigators, thereby

* { mitchell, njoshi, jmb } @robots.ox.ac.uk, emmajhelm@hotmail.com, fgleeson@mac.com

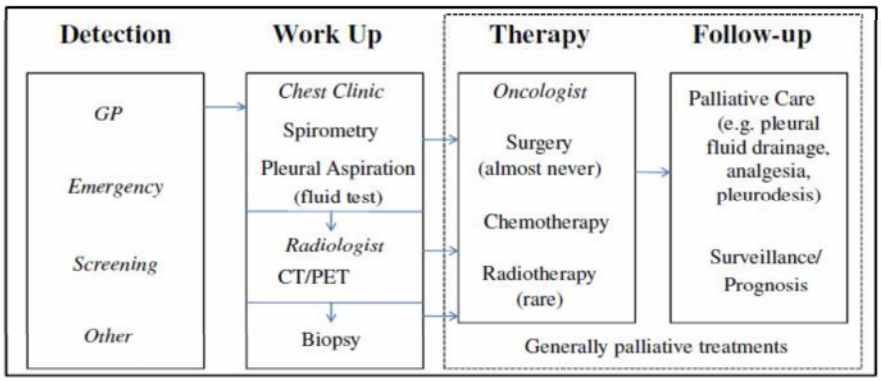

Figure 1. Typical Patient Journey for Mesothelioma

creating unnecessary ambiguity in the measurement. This is largely because of the circumferential, irregular shape and growth pattern of the tumour volume which does not lend itself to description by a unidimensional measurement. For this reason, a modified RECIST [7] has been suggested for use on MPM. In this method, tumour thickness perpendicular to the chest wall or mediastinum is measured in two positions at three separate levels on transverse cuts of the CT scan. The sum of these six measurements is then defined as a single pleural unidimensional measurement. One drawback of this method is that it is known to be prone to inter- and intra-observer variability, especially given the circumferential morphology of MPM tumours. Such difficulties may impair the assessment of treatment response in clinical trials. A study on this variability is given in [5].

Assessment of disease progression in MPM focuses on changes in volume of pleural fluid and tumour and assessment of the underlying lung. Increase in tumour volume results in decreased chest wall compliance and reduced inflation of the underlying lung. Pleural fluid also causes atelectasis (collapse) of underlying lung. In this paper, we report initial developments toward a fully automatic segmentation method to measure changes in MPM. A key component of our method is probability density function (PDF) estimation of intensity values. We report preliminary semi-automatic segmentation results based on the estimated PDFs.

2 Method

2.1 Image Analysis Problem and Challenges

The first stage in assessing disease burden is the separation of tumour from surrounding tissues. Building an image mask to the lungs is crucial to initiate the segmentation. A method of masking the lungs based on modelling the thoracic cavity by connecting the ribs, which appear clearly in CT, was developed in [8]. However, a difficulty with the method derives from the similar pixels intensities between tissues found in close proximity in an image scan (see Fig. 2). Likely interference comes from nearby tissues such as: liver, mediastinum, esophagus and pleural fluid. This effectively rules out the use of thresholding. Moreover, the geometric complexity of tissues presents an additional challenge, since different tissues of similar densities usually form homogeneous structures shown on the images. Therefore propagation-based segmentation algorithms, such as active contours are also less effective in achieving good segmentation.

Instead, we apply a method to estimate the PDFs of intensity values of individual tissues defined by slices of the image volume, following partial segmentation by the clinician. These estimates can then be used to formulate automatic segmentation algorithms. This relatively moderate intervention improves the segmentation process and is considerably more efficient than the current clinical practice. The key is the accuracy of the PDF estimation, since it directly affects the subsequent segmentation step. Evidently, there is a trade-off between having sufficient data to improve the accuracy of PDF estimation versus minimising the amount of manual segmentation required. To achieve this, we perform manual segmentation on just three to five of the 60 to 90 image slices for the regions of interests (ROI); in this case: tumour; aerated lung; fluid; liver; and mediastinum.

2.2 PDF Estimation

PDFs are central to many advanced segmentation and registration techniques. For instance, in image segmentation, each class of the image is associated with an observed likelihood PDF of the image intensity of the class. These PDFs are then used in a Bayesian framework to segment the image accordingly. Another important aspect of the PDFs is that they provide the basis for computing other quantities, such as entropy and mutual information. In this paper, to validate

our findings we present segmentation results based on the estimated PDFs.

A number of PDF estimation methods have been developed. PDF estimation for medical applications increasingly uses non-parametric (NP) methods because for most medical applications, it is not sufficient to assume a parametric form assumption since image noise is typically not Gaussian; anatomical structures are complex and variable; and there are various imaging artefacts. Three such well-known methods are: by histogram; kernel density estimation(KDE) and NP windows (NPW) [9]. Histogram estimation is the most computationally efficient estimator available but accurate PDF estimation requires a large number of data samples. KDE gives better results; but lacks in computational efficiency when optimal bandwidth is required. Estimation using NPW has two notable advantages. First, unlike the histogram method, it requires only a small number of data samples for accurate estimation. Also it is data-driven and does not need any parameters to be set, unlike KDE.

2.3 Implementation of the NPW Estimator

For 2-D individual image slices in a medical data volume, we have two positional variables X_1, X_2, each each representing a coordinate axis. Denote pixel intensity by Y_1. For analytical convenience (i.e construction of a Jacobian), we also introduce a dummy variable Y_2. To find the PDF estimate of Y_1, four different implementation methods have been given in [9]. For illustration, we describe the implementation based on planar approximations. This assumes that the intensity surface is piecewise planar between the region defined by three mutually neighbouring pixels that form a triangle, or a triangular triplet. It has been proven elsewhere [9] that PDF f_{Y_1} of intensity values $y_1$is given by Eqs. 1a-d. Here a,b and c are re-defined coefficients where $a = v_{max} - v_{min}$, $b = v_{mid} - v_{min}$ and $c = v_{min}$ such that $(v_{max}, v_{mid}, v_{min})$ is a triplet set found by rearranging the ordering of three selected intensity values (v_1, v_2, v_3) of vertices. Then by taking the sum of f_{Y_1} over all possible triplets in an image, we are able to obtain the overall PDF representation of the pixels present.

$$f_{Y_1}(y_1) = \begin{cases} \dfrac{2(y_1 - c)}{ab} & \text{for range } c \leq y_1 \leq a + c \text{ when } a, b \neq 0, \quad (1a) \\ \dfrac{2(y_1 - b - c)}{(a - b)b}, & a + c \leq y_1 \leq b + c \text{ when } a, b \neq 0, \quad (1b) \\ \dfrac{2(a + c - y_1)}{a|a|}, & c \leq y_1 \leq a + c;\ a > 0 \text{ and } a + c \leq y_1 \leq c;\ a < 0 \text{ when } a \neq 0, b = 0, \quad (1c) \\ 1, & y_1 = c \text{ or } a + c \text{ when } a, b = 0 \text{ or } a = b. \quad (1d) \end{cases}$$

3 Results

3.1 Data

So far we have analysed serial CT data from four patients undergoing chemotherapy for MPM. All patients have a baseline scan and between 1 and 3 follow up examinations. The CT examinations were performed on a LightSpeed Ultra CT scanner (GE Medical Systems). Each CT scan volume consists of slices of 512 x 512 pixel matrices. An assortment of thick (5mm) and thin (2.5mm) slice scans are available. For reasons to be explained later, only thick slice data volumes have been used so far. The time interval between the sequential scans for the involved patients ranges from 3 to 12 weeks.

3.2 Procedure

Morphological erosion operation is first applied to manual segmentation data to reduce the partial volume effects on tissue boundaries. NPW estimator is then used for individual tissue classes in the eroded 2D image slices in each volume as defined by manual segmentation from the clinician. Then the tissue class PDF estimate for the full volume is found by taking the algebraic average of the corresponding estimates of the 2D image slices. This is a reasonable approximate of the 3D PDF representation because thick-slice scans (resolution: 5mm) have been used in this study, rendering inter-slice interpolation a less effective method for the task. Estimation results are shown in Fig. 2. To evaluate the performance of NPW, we use L-2 norm defined by $L_2 = \sqrt{\Sigma_i (u_{His}(i) - u_{NPW}(i))^2}$ where $u_{His}(i)$ and $u_{NPW}(i)$ are histogram and NPW estimations, respectively. It has been found that the norm is in the order 10^{-4} over the range shown. Compare to an average data value in the order 10^{-3}, we conclude that the error norm between the histogram and NPW estimations is relatively small and falls within the tolerance range. This justifies the accuracy and use of NPW for PDF estimation.

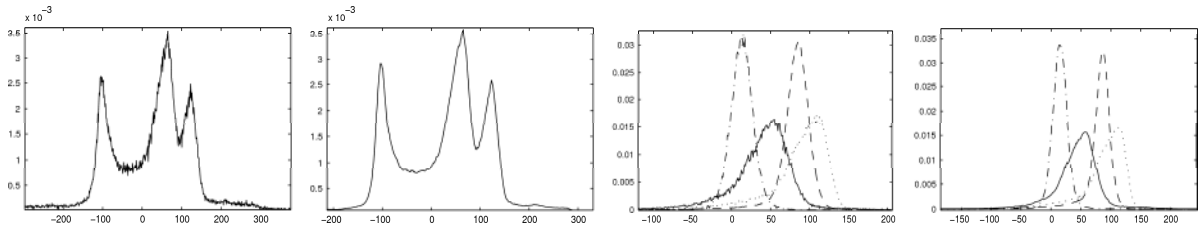

(a) 'unguided' Histogram (b) 'unguided' NPW (c) 'guided' Histogram (d) 'guided' NPW

Figure 2. Comparison of NPW with histogram estimation for an arbitrarily chosen thoracic CT image slice. Note that NPW estimator also offers the advantage of producing smoother estimates. This notably benefits the interpretability of the estimated PDF. Only parts of the overall PDF are shown here to illustrate this point. A number of important tissues such as tumour *(solid)*, fluid *(dot-dash)*, liver *(dash)* and mediastinum *(dot)* are found in this intensity range. Note that all of these tissues are displayed by a single peak in the 'unguided' PDF estimation; this illustrates the difficulties in segmenting the tissues described earlier. This issue is solved with a 'guided' estimation, that is, with the use of manual segmentation data; Here each one of these tissues is represented separately by an independent peak. Unless given otherwise, all plots presented in this paper have DICOM image intensity as the x-axis and PDF height as the y-axis.

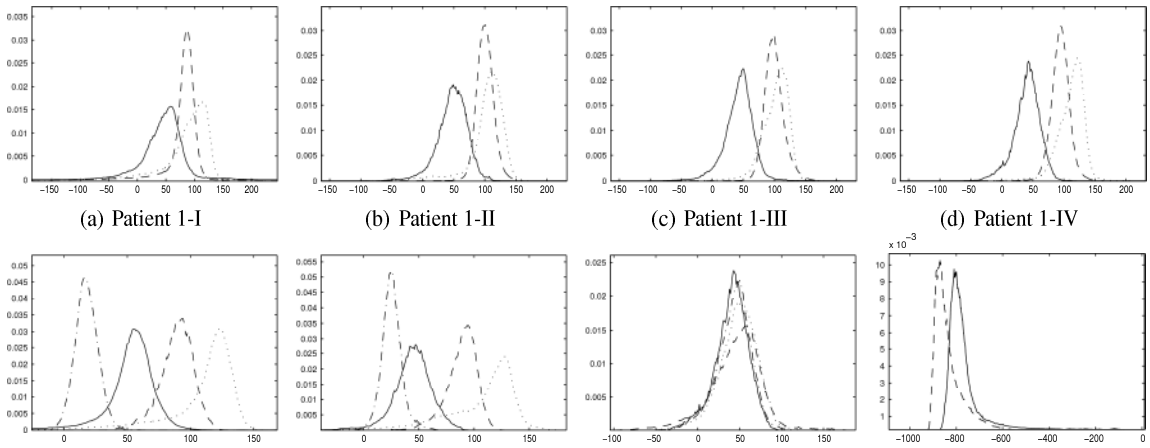

(a) Patient 1-I (b) Patient 1-II (c) Patient 1-III (d) Patient 1-IV

(e) Patient 2-I (f) Patient 2-II (g) Tumour Response (h) Aerated Lung Response

Figure 3. Response assessment for MPM patients. Shown here are tumour *(solid)*, fluid *(dot-dash)*, liver *(dash)* and mediastinum *(dot)*. The tumour and aerated lung responses for Patient 1 are represented by, in the order from early to later stages of the treatment, *dash, dot, dot-dash, solid*.

3.3 Response Assessment

Results from the CT images volumes from two mesothelioma-diagnosed patients are shown in Fig. 3. Assessment of treatment response is performed on each of these patients. The aim is to evaluate the feasibility of automatic segmentation based on these PDF results. Four such studies are carried out on patient 1, one baseline scan and one scan after each chemotherapy cycle. It has been observed that the measured tissues (tumour, liver and mediastinum) are largely unchanged. This can be explained by the fact that treatments have been palliative and have slowed progression of the disease, rather than resulting in significant regression. A comparison of the tumour PDF at different stages for patient 1 is given in Fig. 3g) to illustrate this point further. A key observation is the the image intensities of different tissues shown are found in a relatively narrow range. This suggests that image intensity alone might not be sufficient to produce good segmentation results for most MPM scans.

4 Discussion & Summary

For many individual tissue PDF representations such as those in Fig. 2d), parametric assumption (i.e Gaussian, Poisson) does not hold well. This justifies the use of non-parametric methods such as NP windows for their estimation. In addition, most PDFs show a clear distinction between individual tissue classes. Therefore we are able to segment these images based on the image intensity values. In Fig. 4 we show some initial experiments for semi-automatic segmentation. Here we have used an established level set segmentation method that uses that PDF estimation described earlier [9]. Further experiments with this method are underway. Modified RECIST is less successful in quantifying the progression of thoracic tissues. Therefore volumetric changes will have to be monitored to produce good segmentation.

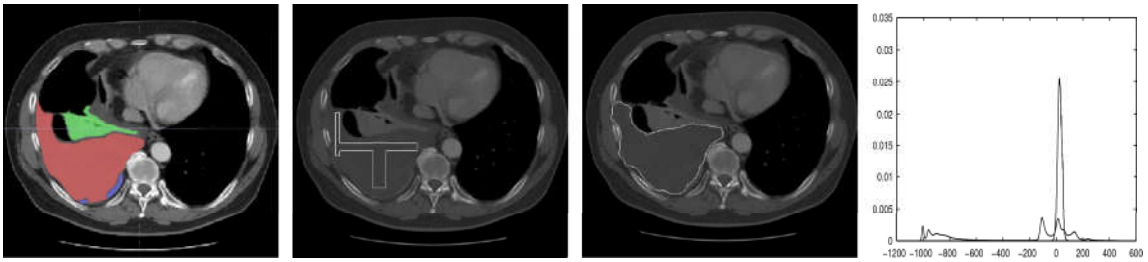

(a) Manual Segmentation (b) Initialisation (c) Segmented Fluid (d) Fluid PDF

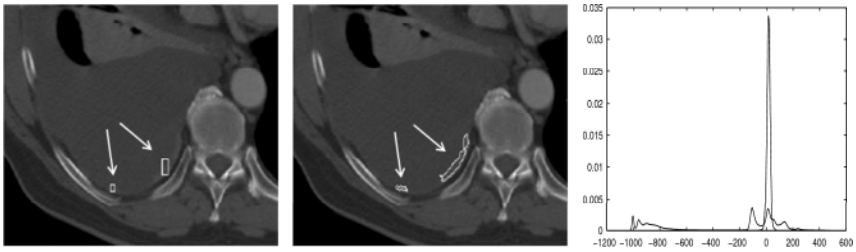

(e) Initialisation (f) Segmented Tumour (g) Tumour PDF

Figure 4. Preliminary segmentation using PDF estimates from Fig. 2d). The PDFs show the comparison of the tissue, P_{in} *(the peak)* against overall PDF, P_{out} *(the base curve)*. By visual inspection it can be noted that the PDF estimates provide a good basis for the segmenting operation as they distinctly separated out the tissue of interest in each of the two cases.

This necessitates the need for volume segmentation. In this paper we made observations on PDFs, predicted a PDF-based segmentation is feasible, as supported by the semi-automatic segmentation results. We also note that to date we have only concentrated on less complex scans with relatively small areas of consolidated lung. For most MPM scans, as already demonstrated by the results, image intensity alone is insufficient to give good segmentations. We are beginning to investigate further the application of the NPW estimator for automatic segmentation. A good starting point is to examine ways with which the manual segmentation is traditionally accomplished. Our study has shown that in addition to image pixel intensities, texture; tissue heterogeneity; and knowledge of normal anatomy may help identify a tissue's presence. Image texture is mostly image technique-dependent and can be a challenge to accurately quantify. Tissue heterogeneity can be measured by information-theoretic entropy $H = -\sum_i P(i) log P(i)$ where $P(i)$ is the probability at value i. Higher entropy values usually mean a more heterogeneous intensity distribution and vice versa. For assessing MPM response to treatment, monitoring the heterogeneity change is another area of good clinical interests. These additional measures might provide good insights into developing a better segmentation algorithm.

Acknowledgements

This ongoing project is funded by GE Medical Systems. Niranjan Joshi and Mike Brady would like to acknowledge funding support from Microsoft Research.

References

1. B. W. Robinson & R. A. Lake. "Advances in malignant mesothelioma." *The New England Journal of Medicine* **15**, pp. 353, 2005.
2. L. Vogel. "Special report: Asbestos in the world." *HESA Newsletter* **27**, 2005.
3. H. Y. Wang & X. R. Zhang. "Advance in clinical diagnosis of mesothelioma of pleura." *Journal of Medical Research, China* **3303**, 2004.
4. N. J. Vogelzang, J. J. Rusthoven, J. Symanowski et al. "Phase iii study of pemetrexed in combination with cisplatin versus cisplatin alone in patients with malignant pleural mesothelioma." *J Clin Oncol* **21**, pp. 2636–2644, 2003.
5. S. G. Armato, J. L. Ogarek, A. Starkey et al. "Variability in mesothelioma tumor response classification." *AJR* **05**, pp. 76, 2005.
6. P. Therass, S. G. Arbuck, E. A. Eisenhauer et al. "New guidelines to evaluate the response to treatment in solid tumors." *J Natl Cancer Inst* **92**, pp. 205–216, 2000.
7. M. J. Byrne & A. K. Nowak. "Modified recist criteria for assessment of response in pleural mesothelioma." *Annals of Oncology* **15**, pp. 257–260, 2004.
8. B. Zhao, L. Schwartz, R. Flores et al. "Automated segmentation of mesothelioma volume on ct scan." In *Proceedings of Medical Imaging: Image Processing*, pp. 866–875. SPIE, 2005.
9. N. Joshi. *Non-parametric Mixture Model based Segmentation of Medical Images*. D.Phil Thesis, Oxford, 2007.